Title

Antennal morphology and sensilla ultrastructure of the malaria vectors, Anopheles maculatus and An. sawadwongporni (Diptera: Culicidae).

Authors

Pusawang, Kanchon
Sriwichai, Patchara
Aupalee, Kittipat
et al.

Publication Date

2023-09-01

DOI

10.1016/j.asd.2023.101296

Peer reviewed

HHS Public Access

Author manuscript

Arthropod Struct Dev. Author manuscript; available in PMC 2024 September 01.

Published in final edited form as:

Arthropod Struct Dev. 2023 September ; 76: 101296. doi:10.1016/j.asd.2023.101296.

Antennal morphology and sensilla ultrastructure of the malaria vectors, *Anopheles maculatus* and *An. sawadwongporni* (Diptera: Culicidae)

Kanchon Pusawang[a], **Patchara Sriwichai**[b], **Kittipat Aupalee**[a], **Thippawan Yasanga**[c], **Rochana Phuackchantuck**[d], **Daibin Zhong**[e], **Guiyun Yan**[e], **Pradya Somboon**[a], **Anuluck Junkum**[a], **Somsakul Pop Wongpalee**[f], **Liwang Cui**[g], **Jetsumon Sattabongkot**[h], **Atiporn Saeung**[a,*]

[a]Graduate Doctoral Degree Program in Parasitology, Faculty of Medicine, Chiang Mai University, Chiang Mai 50200, Thailand.

[b]Department of Medical Entomology, Faculty of Tropical Medicine, Mahidol University, Bangkok 10400, Thailand

[c]Medical Science Research Equipment Center, Faculty of Medicine, Chiang Mai University, Chiang Mai 50200, Thailand

[d]Research Administration Section, Faculty of Medicine, Chiang Mai University, Chiang Mai 50200, Thailand

[e]Department of Population Health and Disease Prevention, University of California, Irvine, CA, 92697, USA

[f]Department of Microbiology, Faculty of Medicine, Chiang Mai University, Chiang Mai 50200, Thailand

[g]Department of Internal Medicine, Morsani College of Medicine, University of South Florida, Tampa, FL, 33612, USA

[*]**Corresponding author email:** atisaeung.noi@gmail.com (A. Saeung).

Authorship Statement

All of the persons who met the authorship criteria are listed as authors, and all of them certified that they participated in the work sufficiently to take public responsibility for the content, including participation in the concept, design, analysis, writing and revision of the manuscript. Furthermore, each author certified that this or similar material has not been submitted to or published in any other publication before its appearance in Arthropod Structure and Development.

CRediT authorship contribution statement

Kanchon Pusawang: Data Curation, Formal analysis, Investigation, Methodology, Writing - original draft, Writing - review & editing. **Patchara Sriwichai:** Methodology, Supervision, Writing-review & editing, Funding acquisition. **Kittipat Aupalee, Thippawan Yasanga, Rochana Phuackchantuck:** Investigation, Methodology, Writing - review & editing. **Daibin Zhong, Guiyun Yan, Pradya Somboon, Anuluck Junkum, Somsakul Pop Wongpalee:** Supervision, Writing-review & editing. **Liwang Cui, Jetsumon Sattabongkot:** Supervision, Writing-review & editing, Funding acquisition. **Atiporn Saeung:** Conceptualization, Formal analysis, Methodology, Writing - original draft, Writing - review & editing.

Declaration of Competing Interest

All of the authors declare no conflict of interest. The funders had no role in the design of the study; collection, analyses or interpretation of data; writing the manuscript or decision to publish the results.

[h]Mahidol Vivax Research Unit, Faculty of Tropical Medicine, Mahidol University, Bangkok 10400, Thailand

Abstract

Mosquitoes rely mainly on the olfactory system to track hosts. Small sensory organs called sensilla contain olfactory neuron receptors that perceive different kinds of odorants and transfer crucial information regarding the surrounding environment. *Anopheles maculatus* and *An. sawadwongporni*, members of the Maculatus Group, are regarded as vectors of *Plasmodium* in Thailand. The fine structure of their sensilla has yet to be identified. Herein, scanning electron microscopy was used to examine the sensilla located on the antennae of adults *An. maculatus* and *An. sawadwongporni*, collected from the Thai-Myanmar border. Four major types of antennal sensilla were discovered in both species: chaetica, coeloconica, basiconica (groove pegs) and trichodea. The antennae of female *An. maculatus* have longer lengths (mean ± SE) in the long sharp trichodea (40.62 ± 0.35 > 38.20 ± 0.36), blunt-tipped trichodea (20.39 ± 0.62 > 18.62 ± 0.35), and basiconica (7.84 ± 0.15 > 7.41 ± 0.12) than those of *An. sawadwongporni*. Using light microscopy, it was found that the mean numbers of large sensilla coeloconica (lco) on both flagella in *An. maculatus* (left: 32.97 ± 0.48; right: 32.27 ± 0.65) are also greater when compared to *An. sawadwongporni* (left: 30.40 ± 0.62; right: 29.97 ± 0.49). The mean counts of lco located on flagellomeres 1–3, 5, 6, and 9 in *An. maculatus* are significantly higher than those of *An. sawadwongporni*. The data in this study indicated that two closely related *Anopheles* species exhibit similar morphology of antenna sensilla types, but show variations in length, and likewise in the number of large sensilla coeloconica between them, suggesting they might be causative factors that affect their behaviors driven by the sense of smell.

Keywords

Scanning electron microscopy; Maculatus Group; Sensory organs

1. Introduction

Despite all efforts to control and eliminate malaria, this disease still poses a significant public health problem globally. In 2021, there were an estimated 619,000 deaths from malaria worldwide, and most of them were reported in children in sub-Saharan Africa (World Health Organization, 2022). One of the vital components that contribute to the spread of the disease is the *Anopheles* mosquito (Macdonald, 1957; Takken and Verhulst, 2013). Females require a blood meal to develop their eggs (Allan et al., 1987), and some of them carry the *Plasmodium* spp. parasites to humans by biting with a long-piercing mouth (proboscis). The predominant anthropophilic malaria vector in Africa is *Anopheles gambiae* (White, 1974), whereas *An. maculatus* and *An. sawadwongporni* are known to play a role in malaria transmission along the Thai-Myanmar border (Sriwichai et al., 2016).

In blood-sucking insects, such as mosquitoes, odors play an essential role in host-seeking behavior along with CO_2, body heat, and even vision (Alonso San Alberto et al., 2022; Coutinho-Abreu et al., 2022). Antennae and maxillary palps of adult female mosquitoes house sensory organs named sensilla (Mclver, 1982). Various receptors located on the

sensilla are used to detect the chemosensory cues, enabling them to precisely locate hosts, oviposition sites, and food. Then, activation of olfactory neurons occurs, and the information is transmitted to olfactory glomeruli within the antennal lobe of the mosquito's brain (Konopka et al., 2021). More broadly, odorant receptors (ORs) respond to esters and alcohols, while ionotropic receptors (IRs) primarily focus on amines and organic acids (Hallem and Carlson, 2006; Knecht et al., 2016). Many researchers found that even genetically engineered mosquitoes lacking an odorant receptor co-receptor (*Orco*) showed moderate attraction to human skin in the presence of CO_2 (DeGennaro et al., 2013). Reduction in attraction to humans was observed in the IR coreceptor mutant (lacking *Ir8a*, *Ir25a*, or *Ir76b*) *Aedes aegypti* (Raji et al., 2019; De Obaldia et al., 2022). Mutating the *Gr3* gene responsible for the CO_2 receptor only reduces attraction in *Ae. aegypti*, but they can still bite human hosts (McMeniman et al., 2014). These results suggest a robust olfactory system in mosquitoes.

There have been several previous publications related to the antennal sensilla of several important mosquito species, including *Ae. aegypti*, *An. gambiae* complex, *An. stephensi*, *An. dirus* complex and *An. minimus* complex (Slifer and Sekhon, 1962; McIver, 1978; McIver and Siemicki, 1979; Pitts and Zwiebel, 2006; Taai et al., 2017, 2019). These studies have identified five distinct types of sensilla: ampullacea, basiconica (grooved peg), coeloconica, chaetica and trichodea, which vary in size and number. However, the fine morphology of sensilla in the Maculatus Group has been elusive and described inadequately. Filling this knowledge gap would provide a better understanding of their taxonomy, evolution and behavior. Our research also serves as a foundation for further studies in olfactory neuroscience. Interfering with the function or expression of olfactory receptors inside the sensilla can diminish mosquito-feeding behavior (McMeniman et al., 2014), leading to new interventions for preventing the transmission of mosquito-borne diseases.

This study aimed to identify key sensilla within morphological-like malaria vectors and classify them into types. Scanning electron and light microscopy were carried out to study the antennal ultrastructure of two field-originated female adults of *An. maculatus* and *An. sawadwongporni* from the Maculatus Group. Furthermore, a comparative study was performed, in order to report differences between species and discuss their probable functions. The antennal sensilla of *An. maculatus* and *An. sawadwongporni* of the Maculatus Group were reported for the first time in the present study.

2. Materials and Methods

2.1 Study site

Anopheles mosquitoes were collected in Suan Oi village, Tha Song Yang district, Tak province (SO, 17° 32' 26.484" N, 97° 56' 16.908" E), a malaria endemic area located along the Thai-Myanmar border. There were 596 residents in the area at that time. Foraging and farming were the main occupations, with most of the area surrounded by forests. According to the Bureau of Vector-Borne Diseases, malaria cases were 262 in 2021. *Plasmodium vivax* was found predominantly, followed by a few cases of *P. falciparum* infection (Ministry of Public Health, 2022). Average temperature and relative humidity were measured by a HOBO weather data logger at 26.02°C and 66.15%, respectively (December). Average monthly

rainfall in Tha Song Yang district was approximately 180 mm during the rainy season (June-October) (Thai Meteorological Department, 2022).

2.2 Mosquito collection

Entomological surveys were conducted in December 2021 and June 2022, when the peak of malaria cases and abundance of mosquitoes soared. Outdoor buffalo-baited collections of adult female *Anopheles* were made on four consecutive nights. At 6.00 p.m., a cow was tethered inside a net tent (3.6 × 3.5 × 2 m), partially left open until next morning at 6.00 a.m. Blood-engorged female mosquitoes resting on inside walls of the net were collected from the cow by an aspirator and placed inside a small net-covered cup. Sugar-soaked cotton was placed on the cup in order to increase humidity and feed the mosquitoes. Then, all of the mosquitoes were transferred to the laboratory for identification.

2.3 Morphological identification

All mosquitoes were identified morphologically by using taxonomic keys developed by Rattanarithikul et al. (2006). Only mosquitoes of the Maculatus Group were used in this study. They were transferred individually into a plastic cup lined with white paper and covered with a transparent net. Each cup was filled with distilled water (1/3 of its volume) as a place for laying eggs. All of the cups were covered with a dark plastic bag to mimic a night environment. After three days, the laid eggs were exposed to a 60-watt light for warming the eggs until hatching. The maternal mosquitoes (F0) were kept in absolute ethanol in a sterile 1.5 ml microcentrifuge tube at 4°C until further analysis. Then, larvae (F1) were reared until they became adults (Choochote and Saeung, 2013).

2.4 Molecular identification with multiplex-PCR assay

Genomic DNA was extracted from the whole body of individual adult females (F0) using the PureLink™ Genomic DNA Mini Kit (Invitrogen, Carlsbad, CA, USA), according to the manufacturer's instructions. DNA quantity was evaluated using Nanodrop 2000 (Desjardins and Conklin, 2010). The ITS2 region of all samples was amplified using the AS-PCR assay with forward primer 5.8F (5'-ATC ACT CGG CTC GTG GAT CG-3') and the specific reverse primer MAC for *An. maculatus* (5'-GAC GGT CAG TCT GGT AAA GT-3'), SAW for *An. sawadwongporni* (5′-ACG GTC CCG CAT CAG GTG C-3′), and PSEU for *An. pseudowillmori* (5′-GCC CCC GGG TGT CAA ACA G-3′) (Walton et al., 2007). Each PCR reaction was carried out in a total of 25 μl volumes containing 0.5 U of *Taq* DNA polymerase, 10X reaction buffer, 2.5 mM of $MgCl_2$, 0.2 mM of each dNTP, 0.2 mM of each primer, and 2 μl of DNA template. The conditions of amplification consisted of initial denaturation at 94°C for 5 min, 35 cycles of denaturation at 94°C for 1 min, annealing at 61°C for 30 s, and extension at 72°C for 30 s, with a final extension at 72°C for 5 min. The amplified products were electrophoresed on 2% agarose gel stained with Ultrapower™ (BioTeke, Bejing, China) dye.

2.5 *Cox1* sequencing

The *cox1* gene of randomly selected DNA samples was amplified using the primer combination LCO1490 (5′-GGT CAA CAA ATC ATA AAG ATA TTG G-3′) and

HCO2198 (5′-TAA ACT TCA GGG TGA CCA AAA AAT CA-3′) (Folmer et al., 1994). Each PCR reaction was conducted in 20 μL volumes containing 1 U of *Taq* DNA polymerase, 2 μL of 10X buffer, 0.2 mM of each dNTP, 0.2 mM of each primer, and 2 μL of DNA template. The PCR program comprised initial denaturation at 94°C for 2 min, 40 cycles of denaturation at 94°C for 30 s, annealing at 45°C for 30 s, and extension at 72°C for 30 s, with a final extension at 72°C for 5 min. The amplified products were electrophoresed on 2% agarose gel and stained using Ultrapower™ (BioTeke, Bejing, China) dye. All *cox1* PCR products showing positive bands were sent for Sanger sequencing at First BASE Laboratories (Selangor, Malaysia).

2.6 Sequence alignments and phylogenetic analyses

The *cox1* sequences of this study were compared with those previously published in GenBank using the standard nucleotide Basic Logical Alignment Search Tool (BLAST), available at https://blast.ncbi.nlm.nih.gov/Blast.cgi. The reference sequences of *An. maculatus* (MK579204.1), *An. sawadwongporni* (MK579214.1), *An. pseudowillmori* (MK579224.1) and *An. dravidicus* (KF406679.1) were included. *Aedes albopictus* (KP843399.1) and *Culex quinquefasciatus* (HQ398883.1) were used as outgroups. Consensus sequences were aligned using MUSCLE under default parameters (Edgar, 2004). Redundant nucleotides at both ends were trimmed. Phylogenetic analyses were conducted using Maximum Likelihood (ML) with MEGA version 7.0 (Kumar et al., 2016). The Kimura 2-parameter (K2P) model and bootstrap analysis with 1,000 replicates were implemented (Kimura, 1980). The most appropriate evolutionary nucleotide model was determined under jModel Test version 2.1.10 (Darriba et al., 2012), which was GTR+I+G.

2.7 Light microscopy

After pupation, newly emerged mosquitoes were allowed three days to accustom themselves to the lab environment. Then healthy adults were selected for experiments. Thirty heads of adult females were observed for large sensilla coeloconica (lco) on each antennal flagellum using an Olympus BX53 compound microscope at 400X magnification (Olympus, BX53, Tokyo). The head of each individual specimen was cut off and placed in a small bottle of 10% potassium hydroxide (KOH) solution, which was then kept in an oven at 45°C for 45 min. Following the clearing steps, the heads were cleaned with 80% ethanol to remove KOH solution. The antennae were extracted gently with an insect needle, and each antenna was mounted on a microscope slide with Neo-Shigaral medium. The large sensilla coeloconica on the left and right flagella of each species were counted and calculated (n = 60/species) (Taai et al., 2017).

2.8 Scanning electron microscopy

Briefly, the heads of three-day-old adult female *An. maculatus* and *An. sawadwongporni* were cut off initially and then rinsed with phosphate buffer saline pH 7.4, immersed in 2.5% glutaraldehyde and placed in an incubator at 4°C for 24 h. After that, the heads were washed twice with phosphate buffer solution for 10 min and subsequently dehydrated through a sequence of ethanol concentrations (twice): 35, 70 and 80% (10 min), and 95% (15 min), followed by absolute ethanol (10 min). Then, the heads were dried in a critical point dryer before mounting and coating their sections on aluminum stubs, by

conductive double-sided carbon tape, and being subsequently sputter-coated using gold particles (Quorum, Q105R Plus, East Sussex) (Huang et al., 2022). The scanning electron microscope (JEOL GmbH, JSM-6610LV, Freising) was used to observe and photograph the antennal sensilla. Identification of sensillum types followed the characteristic terminology described by previous reports (Zacharuk, 1980; Mclver, 1982; Taai et al., 2017; Jatuwattana et al., 2019).

2.9 Data analysis

Student's t-tests were used to determine whether the mean numbers of large sensilla coeloconica per flagellum under a light microscope differ significantly. Statistically significant differences between the mean numbers of large sensilla coeloconica per flagellomere under a light microscope was tested using Mann-Whitney U tests. The total lengths of the antennae, lengths of individual segments, and lengths and basal widths of sensilla were measured using the ImageJ program (Schneider et al., 2012). Differences between each species were compared using the Student's t-test and Mann-Whitney U tests. All data were analyzed and visualized using SPSS version 23.0 for Windows, and R (IBM Corp, 2015; R Core Team, 2022).

2.10 Ethics approval

The protocol for this study was approved by the Research Ethics Committee (Institutional Animal Care and Use Committee) (Protocol Number 16/2019) of the Faculty of Medicine, Chiang Mai University, Chiang Mai province, Thailand.

3. Results

3.1 Mosquito collection and identification

A total of 103 *Anopheles* mosquitoes belonging to species of the Minimus Complex, the Maculatus Group and other *Anopheles* spp. were obtained from Suan Oi village (Fig. 1A). Two species of the Maculatus Group, *An. maculatus* and *An. sawadwongporni*, identified morphologically comprised 57% (59/103) of the total *Anopheles* spp. captured by using the cow-baited method (Fig. 1A). All of them were blood-fed, but only 37 mosquitoes laid eggs. Multiplex-PCR, based on the ITS2 region, was conducted on sampled mosquitoes that generated offspring. According to the results, 21 *An. maculatus* were found with a PCR band of 180 bp, followed by 16 *An. sawadwongporni* (242 bp). The results are in agreement with morphological identification.

3.2 Phylogenetic analyses

Three samples from each species were selected randomly for *cox1* sequencing. The sequences generated have been deposited in the GenBank nucleotide sequence database with accession numbers: OQ363184–OQ363186 for *An. maculatus* and OQ363187– OQ363189 for *An. sawadwongporni*. The sequence length of all specimens is 595 bp for the maximum likelihood tree construction. K2P genetic distances between *An. maculatus* and *An. sawadwongporni* of the Maculatus Group are shown in Fig. 1B. The interspecific and intraspecific divergences are above 6.9%, and less than 3%, respectively, in both groups. Phylogenetic tree revealed that the group of sequences of *An. maculatus* forms a separate

and unique clade from the one with sequences of *An. sawadwongporni* (Fig. 1C). Results from the clear-distinct separation tree correspond with the ITS2 amplification for species identification (Figure not shown).

3.3 Number of large sensilla coeloconica (lco) on antennae

The numbers of large sensilla coeloconica per flagellomere from *An. maculatus* and *An. sawadwongporni* range from 0–10 and 0–8, respectively. *Anopheles maculatus* has greater mean numbers of lco per flagellum (left: 32.97 ± 0.48; right: 32.27 ± 0.65) than *An. sawadwongporni* (left: 30.40 ± 0.62; right: 29.97 ± 0.49), with a significance of $p < 0.05$ (Fig. 3A). The highest mean number of lco (6.92 ± 0.14) occurs on the first flagellomere in *An. maculatus*, but on the second in *An. sawadwongporni*, which presents the most (6.02 ± 0.11). In addition, the mean numbers of lco on flagellomeres 1–3, 6 and 9 of *An. maculatus* (Fig. 2A, C, E) are significantly greater than those of *An. sawadwongporni*, while there are fewer numbers on flagellomere 5 ($p < 0.05$) (Fig. 3B and Table S2). No lco is found on flagellomeres 11–13 of either species, except for flagellomere 13 of *An. maculatus*, where they are rarely observed (Table S2).

3.4 General morphology of the antennae

The antennae of female *An. maculatus* and *An. sawadwongporni* are morphologically similar, and consist of a basal scape, pedicel and long terminal flagellum (Fig. 5A). The scape (Sc) is collar-shaped and attached behind the pedicel (Pe). The Pe is a fat-round, cup-shaped segment containing Johnston's organ and provided with attachment of the flagellum. Each flagellum comprises 13 flagellomeres (Fig. 4). The Sc, Pe and first flagellomere surface is covered densely with aculeae (ac: microtrichium-like spicules), which decrease gradually from the proximal to distal end of each flagellomere (Fig. 6E). They are seen on the first three flagellomeres and invisible in the following segments until the end.

3.5 Types of sensilla on the antennae

There are four main types of sensilla on the antennae of *An. maculatus* and *An. sawadwongporni*: sensilla chaetica (ch), sensilla trichodea (tc), sensilla coeloconica (sco) and sensilla basiconica (sb) or grooved pegs (Fig. 5B). The morphology of these types shows similarity in both groups. Sensilla chaetica are long, thick-walled seta set in sturdy sockets (alveoli). There are large and small subtypes. The large sensilla chaetica (lch) are arranged primarily on a whorl of approximately seven sensilla at the base of flagellomeres 2–13 in both species. The average lengths of large sensilla chaetica are 159.19 ± 6.74 and 156.69 ± 8.89 μm in *An. maculatus* and *An. sawadwongporni*, respectively. The small sensilla chaetica (sch) occur on the distal ends of flagellomeres 2–13. Both subtypes also exist with aculeae on the ventral surface of the first flagellomere. *Anopheles maculatus* and *An. sawadwongporni* display 43.59 ± 2.64 and 42.38 ± 2.69 μm, respectively, in the mean lengths of small sensilla chaetica.

Sensilla trichodea have a finger- or hair-like sensory structure without arising from an alveolus (Fig. 5B, 6F). They are the predominant sensillum on flagellomeres 2–13 of both species. Three subtypes of sensilla trichodea are identified based on length and shape: long sharp trichodea (ltc), short sharp trichodea (stc) and blunt-tipped trichodea (btc). Short sharp

trichodea are fewer in number than the long-sharp trichodea on the flagellum. In comparison to long sharp trichodea, blunt-tipped trichodea do not taper at the tip. These sensilla are closer in length than sharp trichodea. Blunt-tipped trichodea emerge in smaller numbers and are absent on the first flagellomere of both species. The lengths of long-sharp trichodea average 40.62 ± 0.35 and 38.20 ± 0.36 μm in *An. maculatus* and *An. sawadwongporni*, respectively. In general, short sharp trichodea display a longer mean length than blunt-tipped trichodea. The mean lengths of short sharp trichodea are 23.21 ± 0.51 and 22.14 ± 0.63 μm in *An. maculatus* and *An. sawadwongporni*, respectively. For blunt-tipped trichodea, the mean lengths are 20.39 ± 0.62 and 18.62 ± 0.35 μm, respectively.

Sensilla coeloconica (co) are small, thick-walled sensilla, commonly called pitted pegs, borne in a cup-like depression of the antennal wall. The most abundant subtype of this sensilla is large sensilla coeloconica (lco) (Fig. 5B, 6A, 6F). The pegs might project through the circular openings at the surface of the cuticle, and their surfaces are deep-grooved lengthwise. The prevalence of large sensilla coeloconica from scanning electron microscopy results correspond with observations from a compound light microscope in both species. The average circumferences are 15.29 ± 0.27 and 14.71 ± 0.39 μm in *An. maculatus* and *An. sawadwongporni*, respectively. Another less common subtype, small sensilla coeloconica (sco) (Fig. 6B, 6C, 6E), has a peg at the bottom of a pit with a small cuticular opening. Hence the peg is concealed. This type of sensillum is found often on the distal end of flagellomere 1 and the tip of the last (13^{th}) flagellomere. *An. maculatus* and *An. sawadwongporni* have an average circumference of 3.27 ± 0.49 and 2.91 ± 0.17 μm, respectively.

Sensilla basiconica (sb, grooved pegs) are more curved with a peg-like structure (Fig. 5B, 6D). They arise from slightly raised alveoli. Their surfaces resemble sensilla coeloconica, but their grooves are narrower. Sensilla basiconica are predominantly observed on flagellomeres 3–13. Their lengths average 7.84 ± 0.15 and 7.41 ± 0.12 μm in *An. maculatus* and *An. sawadwongporni*, respectively.

3.6 Comparing the mean lengths of flagellomeres, and mean lengths and basal widths of sensilla

There is no difference in the length of each individual flagellomere between *An. maculatus* and *An. sawadwongporni* ($p > 0.05$). However, the mean lengths and mean basal widths of some types of sensilla are found to be significantly different. The mean lengths of long sharp trichodea, blunt-tipped trichodea and sensilla basiconica in *An. maculatus* are significantly longer than those of *An. sawadwongporni* ($p < 0.05$) (Fig. 7). Most of the mean basal widths of sensilla between these two groups do not differ significantly, except for large sensilla chaetica, which are wider in *An. maculatus* ($p = 0.003$).

4. Discussion

Current studies have shown that the Maculatus Group includes at least 10 species (Harbach, 2023). Among these, *An. maculatus* and *An. sawadwongporni* are invovled in malaria transmission along the Thai-Myanmar border (Morgan et al., 2013). The two species are found to harbor a human-infective stage (sporozoite) of malaria in field settings (Sriwichai

et al., 2016, 2017; Sumruayphol et al., 2020). We did not find *An. pseudowillmori*, a malaria vector belonging to the Maculatus Group, in this area during our study period. This might be due to species composition and seasonal dynamics (Sumruayphol et al., 2020). Although the morphological characteristics between *An. maculatus* and *An. sawadwongporni* are relatively similar, these were distinguished successfully at the species level by conducting amplification of the internal transcribed spacer 2 (ITS2) region and cytochrome c oxidase subunits 1 (*cox1*) of mitochondrial DNA sequencing. These results agree with other mosquito phylogenetic studies that used the *cox1* gene as a DNA barcoding marker to identify cryptic mosquito species as well as evolutionary relationships (Ali et al., 2019; Phanitchakun et al., 2019; Wilai et al., 2020).

In this study, four classes of sensilla were observed on the antennae of *An. maculatus* and *An. sawadwongporni*. They looked morphologically indistinguishable between both groups. Nonetheless, using ImageJ to determine the differences in length and width helped in recognizing dissimilarity. Based on results, the long sharp trichodea, blunt-tipped trichodea and sensilla basiconica in *An. maculatus* were remarkably longer than in *An. sawadwongporni*. No difference in the length of each flagellomere was found between species. It should be noted that the average length of five flagella was employed for each measurement. In addition, the mean number of large sensilla coeloconica found in *An. maculatus* was higher. When comparing to other primary malaria vector studies in Thailand, the quantitative observations obtained from this study were greater than those of *An. minimus* (26.25) and *An. dirus* (25.33) (Taai et al., 2017, 2019). Yet *An. minimus* is known to be a superior vector when it comes to human attractiveness (Edwards et al., 2019). This leads to the question of whether the variance in number of antennal sensilla affects the biting behavior among vector species.

Sensilla are the basic compartment of the mosquito peripheral olfactory system, where olfactory receptor neurons (ORNs) are located. Besides the antenna, the set of sensilla is present in the maxillary palps, and labella at the tip of the proboscis (Mclver, 1982). Their numbers and locations vary between sexes (Riabinina et al., 2016). Normally, *Anopheles* antennae bear five types of sensilla as previously stated. Sensilla trichodea were the most common type of sensilla found in this study. Their densities in *An. maculatus* and *An. sawadwongporni* appeared to be similar. With length and shape variations, they were classified into three distinct subtypes (long sharp, short sharp and blunt-tipped trichodea). There are six functional subtypes of sensilla trichodea in *An. gambiae*, based on electrophysiological responses (Qiu et al., 2006). Each trichoid sensillum is innervated by two olfactory neurons that can express ORs and IRs (Mclver, 1982). ORs only have one coreceptor (*Orco*), which is highly conserved among insect species (Rinker et al., 2013). IRs and one of three conserved coreceptors (*IRco: IR8a, IR25a* and *IR76b*) form several subunits that respond to specific odorant ligands (Sparks et al., 2018). Moreover, neurons in each trichoid are found to be stimulated by carboxylic acids (Meijerink and van Loon, 1999), which emanate from human skin and correlate with an elevated preference for humans (De Obaldia et al., 2022). Given that sensilla trichodea are similar morphologically, but might be distinguished by their physiological properties, suggests that single sensillum electrophysiological assays should be conducted to determine the response of each trichoid

to stimuli. Other sensilla types have not been studied as extensively in mosquitoes as sensilla trichodea.

Sensilla basiconica or grooved pegs are seemingly the second most numerous antennal sensilla of *An. maculatus* and *An. sawadwongporni*. They have been involved in host-seeking behavior and responded reliably to lactic acid and ammonia, which are mosquito attractants given off from human breath and skin (Acree Jr et al., 1968; Davis and Sokolove, 1976; Geier et al., 1999; Meijerink et al., 2001). From behavioral study, the combination of ammonia, lactic acid and carboxylic acids produce a synergistic effect that drove human attractiveness in *An. gambiae* (Smallegange et al., 2005). Sensilla basiconica are distinguished morphologically and functionally into two subtypes: short and long sensilla basiconica and only short sensilla basiconica bear lactic acid-excited cells (Bowen, 1995). Three subtypes (I, II, III) and clusters of type III, which interspersed with large sensilla coeloconica, are reported in two species members of the Hyrcanus Group: *An. argyropus* and *An. peditaeniatus* (Wijit et al., 2016; Hempolchom et al., 2017). In this study, sensilla basiconica were homogeneous in shape within species and corresponded to type I, as previously reported by Hempolchom et al. (2017). It can therefore be assumed that significantly greater mean lengths of sensilla basiconica, long sharp and blunt-tipped trichodea, respond to sweat-borne substances derived from humans, and might enhance the host-searching mechanism and other odor-driven behaviors in *An. maculatus*.

Small sensilla coeloconica on the tip of the antenna (flagellomere 13) are innervated by three sensory neurons that contain thermosensory receptors, such as *IR21a* (Gingl et al., 2005; Ni et al., 2016; Greppi et al., 2020). This ionotropic receptor is essential for responding to a temperature shift and heat-seeking behavior. A recent study on *An. gambiae* revealed the presence of *Ir93a*, which is a requisite for humidity and temperature detections, in large sensilla coeloconica, sensilla ampullacea, and also sensilla trichodea (Laursen et al., 2023). Surprisingly, sensilla ampullacea (slit-like openings with small pedicular pegs) were not found in female *An. maculatus* or *An. sawadwongporni* antennae. This sensillum type is present in small numbers and mostly observed on the first flagellomere. In accord with the present results, Hempolchom et al. (2017) demonstrated four types of sensilla with the absence of sensilla ampullacea on the antennae of the eight *Anopheles* species from the Hyrcanus Group. Nevertheless, sensilla ampullacea are associated putatively with the thermosensory pathway (Laursen et al., 2023).

Both long and short subtypes of sensilla chaetica have been implicated as mechanoreceptive/proprioceptive receptors in mosquitoes and are thought to perceive different tactile and vibrational cues through their basic structure (Schneider, 1964; Konopka et al., 2021). These non-olfactory sensilla might also support the inner frame against wind currents (Mclver, 1982). They are present commonly in fewer numbers than sensilla trichoidea (Pitts and Zwiebel, 2006). The fine external structure of sensilla chaetica showed a lack of dendritic neurons and response to mechanical vibrations such as pressure and gravitational force (Keil and Steinbrecht, 1984).

Overall, these data demonstrate similar morphology of the antennal sensilla of two closely related *Anopheles* species; *An. maculatus* and *An. sawadwongporni*. However,

the divergences between sensillum lengths and numbers of large sensilla coeloconica of *An. maculatus* and *An. sawadwongporni* were observed in some flagellomeres. It is still debatable whether those morphological differences have a prominent impact on mosquito preference. Since *An. maculatus* is more competent at malaria transmission than its counterparts, it is important to consider the potential for *Plasmodium* to manipulate vector behavior (Stanczyk et al., 2017). Indeed, laboratory findings uncovered the behavioral alterations of mosquitoes carrying the transmissible sporozoite stage, such as increased attraction to human odors in *P. falciparum*-infected *An. gambiae* females (Smallegange et al., 2013). The concrete role of each sensillum in the Maculatus Group, which contributes to biting behavior and spread of disease, also remains to be seen. Taken together, determining how mosquitoes with similar morphological and bio-ecological characteristics adjust their olfactory system is of interest, and these data may provide a new leap in vector control strategies.

5. Conclusion

Examination of the sensilla in *An. maculatus* and *An. sawadwongporni* provides a valuable starting point for further studies on the morphology and functions of these crucial sensory organs in mosquitoes. The antennal sensilla of these mosquitoes present almost identical morphological features. Nevertheless, the differences between the lengths of certain sensilla in both species have been discerned. Therefore, it is possible that they could potentially influence their olfactory-driven behavior and vector competence. Further research should be undertaken to investigate the exact role of each sensillum as a part of host-seeking modalities, thus offering cutting-edge implementations of integrated vector management.

Supplementary Material

Refer to Web version on PubMed Central for supplementary material.

Funding

This research was funded by the National Institutes of Health, USA (U19AI089672 to L. Cui and D43TW006571 to J. Sat). It was supported partially by Specific League Funds from Mahidol University to P. Sriwichai. The authors acknowledge funding from the Royal Golden Jubilee Ph.D. program (PHD/0113/2560) to K. Pusawang and A. Saeung.

References

Acree F Jr, Turner R, Gouck H, Beroza M, Smith N, 1968. L-Lactic acid: a mosquito attractant isolated from humans. Science 161, 1346–1347. [PubMed: 5673445]

Ali RSM, Wahid I, Saeung A, Wannasan A, Harbach RE, Somboon P, 2019. Genetic and morphological evidence for a new species of the Maculatus Group of *Anopheles* subgenus *Cellia* (Diptera: Culicidae) in Java, Indonesia. Parasit. Vectors 12, 107. [PubMed: 30871633]

Allan SA, Day JF, Edman JD, 1987. Visual ecology of biting flies. Annu. Rev. Entomol 32, 297–314. [PubMed: 2880551]

Alonso San Alberto D, Rusch C, Zhan Y, Straw AD, Montell C, Riffell JA, 2022. The olfactory gating of visual preferences to human skin and visible spectra in mosquitoes. Nat. Commun 13, 555. [PubMed: 35121739]

Bowen M, 1995. Sensilla basiconica (grooved pegs) on the antennae of female mosquitoes: electrophysiology and morphology. Entomol. Exp. Appl 77, 233–238.

Choochote W, Saeung A, 2013. Systematic techniques for the recognition of Anopheles species complexes. In: Manguin S (Ed.), *Anopheles* Mosquitoes-New Insights Into Malaria Vectors. Intech, pp. 57–79.

Coutinho-Abreu IV, Riffell JA, Akbari OS, 2022. Human attractive cues and mosquito host-seeking behavior. Trends Parasitol. 38, 246–264. [PubMed: 34674963]

Darriba D, Taboada GL, Doallo R, Posada D, 2012. jModelTest 2: more models, new heuristics and parallel computing. Nat. Methods 9, 772–772.

Davis EE, Sokolove PG, 1976. Lactic acid-sensitive receptors on the antennae of the mosquito, *Aedes aegypti*. J. Comp. Physiol 105, 43–54.

De Obaldia ME, Morita T, Dedmon LC, Boehmler DJ, Jiang CS, Zeledon EV, Cross JR, Vosshall LB, 2022. Differential mosquito attraction to humans is associated with skin-derived carboxylic acid levels. Cell 185, 4099–4116. e4013. [PubMed: 36261039]

DeGennaro M, McBride CS, Seeholzer L, Nakagawa T, Dennis EJ, Goldman C, Jasinskiene N, James AA, Vosshall LB, 2013. *orco* mutant mosquitoes lose strong preference for humans and are not repelled by volatile DEET. Nature 498, 487–491. [PubMed: 23719379]

Desjardins P, Conklin D, 2010. NanoDrop microvolume quantitation of nucleic acids. J. Vis. Exp 45, 1–4. e2565.

Edgar RC, 2004. MUSCLE: multiple sequence alignment with high accuracy and high throughput. Nucleic Acids Res. 32, 1792–1797. [PubMed: 15034147]

Edwards HM, Sriwichai P, Kirabittir K, Prachumsri J, Chavez IF, Hii J, 2019. Transmission risk beyond the village: entomological and human factors contributing to residual malaria transmission in an area approaching malaria elimination on the Thailand–Myanmar border. Malar. J 18, 221. [PubMed: 31262309]

Folmer O, Black M, Hoeh W, Lutz R, Vrijenhoek R, 1994. DNA primers for amplification of mitochondrial cytochrome c oxidase subunit I from diverse metazoan invertebrates. Mol. Mar. Biol. Biotechnol 3, 294–299. [PubMed: 7881515]

Geier M, Bosch OJ, Boeckh J, 1999. Ammonia as an attractive component of host odour for the yellow fever mosquito, *Aedes aegypti*. Chem. Senses 24, 647–653. [PubMed: 10587497]

Gingl E, Hinterwirth A, Tichy H, 2005. Sensory representation of temperature in mosquito warm and cold cells. J. Neurophysiol 94, 176–185. [PubMed: 15673550]

Greppi C, Laursen WJ, Budelli G, Chang EC, Daniels AM, Van Giesen L, Smidler AL, Catteruccia F, Garrity PA, 2020. Mosquito heat seeking is driven by an ancestral cooling receptor. Science 367, 681–684. [PubMed: 32029627]

Hallem EA, Carlson JR, 2006. Coding of odors by a receptor repertoire. Cell 125, 143–160. [PubMed: 16615896]

Harbach RE, 2023. *Anopheles* classification. https://mosquito-taxonomic-inventory.myspecies.info/node/11358 (accessed 18 May 2023).

Hempolchom C, Yasanga T, Wijit A, Taai K, Dedkhad W, Srisuka W, Thongsahuan S, Otsuka Y, Takaoka H, Saeung A, 2017. Scanning electron microscopy of antennal sensilla of the eight *Anopheles* species of the Hyrcanus Group (Diptera: Culicidae) in Thailand. Parasitol. Res 116, 143–153. [PubMed: 27752768]

Huang F, Srisuka W, Aupalee K, Yasanga T, Phuackchantuck R, Pitasawat B, Junkum A, Limsopatham K, Sanit S, Saingamsook J, Takaoka H, Saeung A, 2022. Ultrastructure of sensilla on the antennae and maxillary palpi of the human-biting black flies, *Simulium nigrogilvum* and *Simulium umphangense*,(Diptera: Simuliidae) in Thailand. Acta Trop. 232, 106494. [PubMed: 35508270]

IBM Corp, 2015. IBM SPSS statistics for windows, version 23.0. Armonk, NY: IBM Corp.

Keil TA, Steinbrecht RA, 1984. Mechanosensitive and olfactory sensilla of insects, Insect Ultrastructure: Volume 2. Springer, pp. 477–516.

Kimura M, 1980. A simple method for estimating evolutionary rates of base substitutions through comparative studies of nucleotide sequences. J. Mol. Evol 16, 111–120. [PubMed: 7463489]

Knecht ZA, Silbering AF, Ni L, Klein M, Budelli G, Bell R, Abuin L, Ferrer AJ, Samuel AD, Benton R, Garrity PA, 2016. Distinct combinations of variant ionotropic glutamate receptors mediate thermosensation and hygrosensation in *Drosophila*. Elife 5, e17879. [PubMed: 27656904]

Konopka JK, Task D, Afify A, Raji J, Deibel K, Maguire S, Lawrence R, Potter CJ, 2021. Olfaction in *Anopheles* mosquitoes. Chem. Senses 46, bjab021.

Kumar S, Stecher G, Tamura K, 2016. MEGA7: molecular evolutionary genetics analysis version 7.0 for bigger datasets. Mol. Biol. Evol 33, 1870–1874. [PubMed: 27004904]

Laursen WJ, Budelli G, Tang R, Chang EC, Busby R, Shankar S, Gerber R, Greppi C, Albuquerque R, Garrity PA, 2023. Humidity sensors that alert mosquitoes to nearby hosts and egg-laying sites. Neuron 111, 874–887. [PubMed: 36640768]

Macdonald G, 1957. The epidemiology and control of malaria. Oxford University Press.

McIver S, 1978. Structure of sensilla trichodea of female *Aedes aegypti* with comments on innervation of antennal sensilla. J. Insect Physiol 24, 383–390.

McIver S, Siemicki R, 1979. Fine structure of antennal sensilla of male *Aedes aegypti* (L.). J. Insect Physiol 25, 21–28.

Mclver SB, 1982. Sensilla of mosquitoes (Diptera: Culicidae). J. Med. Entomol 19, 489–535. [PubMed: 6128422]

McMeniman CJ, Corfas RA, Matthews BJ, Ritchie SA, Vosshall LB, 2014. Multimodal integration of carbon dioxide and other sensory cues drives mosquito attraction to humans. Cell 156, 1060–1071. [PubMed: 24581501]

Meijerink J, Braks M, Van Loon J, 2001. Olfactory receptors on the antennae of the malaria mosquito *Anopheles gambiae* are sensitive to ammonia and other sweat-borne components. J. Insect Physiol 47, 455–464. [PubMed: 11166310]

Ministry of Public Health, 2022. The Status of Malaria Cases in Thailand. http://malaria.ddc.moph.go.th/malariaR10/index_newversion.php (accessed 20 December 2022).

Meijerink J, van Loon JJ, 1999. Sensitivities of antennal olfactory neurons of the malaria mosquito, *Anopheles gambiae*, to carboxylic acids. J. Insect Physiol 45, 365–373. [PubMed: 12770362]

Morgan K, Somboon P, Walton C, 2013. Understanding *Anopheles* diversity in Southeast Asia and its applications for malaria control. In: Manguin S (Ed.), *Anopheles* Mosquitoes-New Insights Into Malaria Vectors. Intech, pp. 327–355.

Ni L, Klein M, Svec KV, Budelli G, Chang EC, Ferrer AJ, Benton R, Samuel AD, Garrity PA, 2016. The ionotropic receptors IR21a and IR25a mediate cool sensing in *Drosophila*. Elife 5, e13254. [PubMed: 27126188]

Phanitchakun T, Namgay R, Miyagi I, Tsuda Y, Walton C, Harbach RE, Somboon P, 2019. Morphological and molecular evidence for a new species of *Lutzia* (Diptera: Culicidae: Culicini) from Thailand. Acta Trop. 191, 77–86. [PubMed: 30593818]

Pitts RJ, Zwiebel LJ, 2006. Antennal sensilla of two female anopheline sibling species with differing host ranges. Malar. J 5, 26. [PubMed: 16573828]

Qiu YT, van Loon JJ, Takken W, Meijerink J, Smid HM, 2006. Olfactory coding in antennal neurons of the malaria mosquito, *Anopheles gambiae*. Chem. Senses 31, 845–863. [PubMed: 16963500]

R Core Team, 2022. R: A Language and Environment for Statistical Computing; R Foundation for Statistical Computing. http://www.R-project.org/ (accessed on 10 December 2022).

Raji JI, Melo N, Castillo JS, Gonzalez S, Saldana V, Stensmyr MC, DeGennaro M, 2019. *Aedes aegypti* mosquitoes detect acidic volatiles found in human odor using the IR8a pathway. Curr. Biol 29, 1253–1262. e1257. [PubMed: 30930038]

Rattanarithikul R, Harrison BA, Panthusiri P, Peyton E, Coleman RE, 2006. Illustrated keys to the mosquitoes of Thailand III. Genera Aedeomyia, Ficalbia, Mimomyia, Hodgesia, Coquillettidia, Mansonia, and Uranotaenia. Southeast Asian J. Trop. Med. Public Health 37, 1.

Riabinina O, Task D, Marr E, Lin CC, Alford R, O'brochta DA, Potter CJ, 2016. Organization of olfactory centres in the malaria mosquito *Anopheles gambiae*. Nat. Commun 7, 13010. [PubMed: 27694947]

Rinker DC, Zhou X, Pitts RJ, Rokas A, Zwiebel LJ, 2013. Antennal transcriptome profiles of anopheline mosquitoes reveal human host olfactory specialization in *Anopheles gambiae*. BMC Genomics 14, 1–15. [PubMed: 23323973]

Schneider CA, Rasband WS, Eliceiri KW, 2012. NIH Image to ImageJ: 25 years of image analysis. Nat. Methods 9, 671–675. [PubMed: 22930834]

Schneider D, 1964. Insect antennae. Annu. Rev. Entomol 9, 103–122.

Slifer EH, Sekhon SS, 1962. The fine structure of the sense organs on the antennal flagellum of the yellow fever mosquito *Aedes aegypti* (Linnaeus). J. Morphol 111, 49–67. [PubMed: 13913860]

Smallegange RC, Qiu YT, van Loon JJ, Takken W, 2005. Synergism between ammonia, lactic acid and carboxylic acids as kairomones in the host-seeking behaviour of the malaria mosquito *Anopheles gambiae* sensu stricto (Diptera: Culicidae). Chem. Senses 30, 145–152. [PubMed: 15703334]

Smallegange RC, van Gemert G-J, van de Vegte-Bolmer M, Gezan S, Takken W, Sauerwein RW, Logan JG, 2013. Malaria infected mosquitoes express enhanced attraction to human odor. PLoS One 8, e63602. [PubMed: 23691073]

Somboon P, Aramrattana A, Lines J, Webber R, 1998. Malaria transmission in relation to population movements in forest areas of norther-west Thailand. Southeas Asian J. Trop. Med. Public Health, 29, 3–9.

Sparks JT, Botsko G, Swale DR, Boland LM, Patel SS, Dickens JC, 2018. Membrane proteins mediating reception and transduction in chemosensory neurons in mosquitoes. Front. Physiol 9, 1309. [PubMed: 30294282]

Sriwichai P, Karl S, Samung Y, Kiattibutr K, Sirichaisinthop J, Mueller I, Cui L, Sattabongkot J, 2017. Imported *Plasmodium falciparum* and locally transmitted *Plasmodium vivax*: cross-border malaria transmission scenario in northwestern Thailand. Malar. J 16, 258. [PubMed: 28637467]

Sriwichai P, Samung Y, Sumruayphol S, Kiattibutr K, Kumpitak C, Payakkapol A, Kaewkungwal J, Yan G, Cui L, Sattabongkot J, 2016. Natural human *Plasmodium* infections in major *Anopheles* mosquitoes in western Thailand. Parasit. Vectors 9, 17. [PubMed: 26762512]

Stanczyk NM, Mescher MC, De Moraes CM, 2017. Effects of malaria infection on mosquito olfaction and behavior: extrapolating data to the field. Curr. Opin. Insect Sci 20, 7–12. [PubMed: 28602239]

Sumruayphol S, Chaiphongpachara T, Samung Y, Ruangsittichai J, Cui L, Zhong D, Sattabongkot J, Sriwichai P, 2020. Seasonal dynamics and molecular differentiation of three natural *Anopheles* species (Diptera: Culicidae) of the Maculatus group (Neocellia series) in malaria hotspot villages of Thailand. Parasit. Vectors 13, 1–11. [PubMed: 31900233]

Taai K, Harbach RE, Aupalee K, Srisuka W, Yasanga T, Otsuka Y, Saeung A, 2017. An effective method for the identification and separation of *Anopheles minimus*, the primary malaria vector in Thailand, and its sister species *Anopheles harrisoni*, with a comparison of their mating behaviors. Parasit. Vectors 10, 1–9. [PubMed: 28049510]

Taai K, Harbach RE, Somboon P, Sriwichai P, Aupalee K, Srisuka W, Yasanga T, Phuackchantuck R, Jatuwattana W, Pusawang K, Saeung A, 2019. A method for distinguishing the important malaria vectors *Anopheles dirus* and *An. cracens* (Diptera: Culicidae) based on antennal sensilla of adult females. Trop. Biomed 36, 926–937. [PubMed: 33597464]

Takken W, Verhulst NO, 2013. Host preferences of blood-feeding mosquitoes. Annu. Rev. Entomol 58, 433–453. [PubMed: 23020619]

Thai Meteorological Department, 2022. Thailand Monthly Rainfall 2022. https://data.tmd.go.th/api/ThailandMonthlyRainfall/v1/index.php?uid=api&ukey=api12345 (accessed 4 December 2022).

Walton C, Somboon P, O'Loughlin SM, Zhang S, Harbach RE, Linton YM, Chen B, Nolan K, Duong S, Fong MY, Vythilingum I, Mohammed ZD, Trung HD, Butlin RK, 2007. Genetic diversity and molecular identification of mosquito species in the *Anopheles maculatus* group using the ITS2 region of rDNA. Infect. Genet. Evol 7, 93–102. [PubMed: 16782411]

White G, 1974. *Anopheles gambiae* complex and disease transmission in Africa. Trans. R. Soc. Trop. Med. Hyg 68, 278–298. [PubMed: 4420769]

Wijit A, Taai K, Dedkhad W, Hempolchom C, Thongsahuan S, Srisuka W, Otsuka Y, Fukuda M, Saeung A, 2016. Comparative studies on the stenogamous and eurygamous behavior of eight *Anopheles* species of the Hyrcanus Group (Diptera: Culicidae) in Thailand. Insects 7, 11. [PubMed: 27023618]

Wilai P, Namgay R, Made Ali RS, Saingamsook J, Saeung A, Junkum A, Walton C, Harbach RE, Somboon P, 2020. A multiplex PCR based on mitochondrial COI sequences for identification of members of the *Anopheles barbirostris* complex (Diptera: Culicidae) in Thailand and other countries in the region. Insects 11, 409. [PubMed: 32630637]

World Health Organization, 2022. World Malaria Report 2022. https://www.who.int/teams/global-malaria-programme/reports/world-malaria-report-2022 (accessed 20 December 2022).

Zacharuk RY, 1980. Ultrastructure and function of insect chemosensilla. Annu. Rev. Entomol 25, 27–47.

Highlights

- The antennal sensilla of *An. maculatus* and *An. sawadwongporni* are reported for the first time.
- The average number of large sensilla coeloconica on *An. maculatus* antennae is greater than those of the latter species under the light microscope.
- The mean lengths of long sharp trichodea, blunt-tipped trichodea, and sensilla basiconica are also significantly longer in *An. maculatus*.

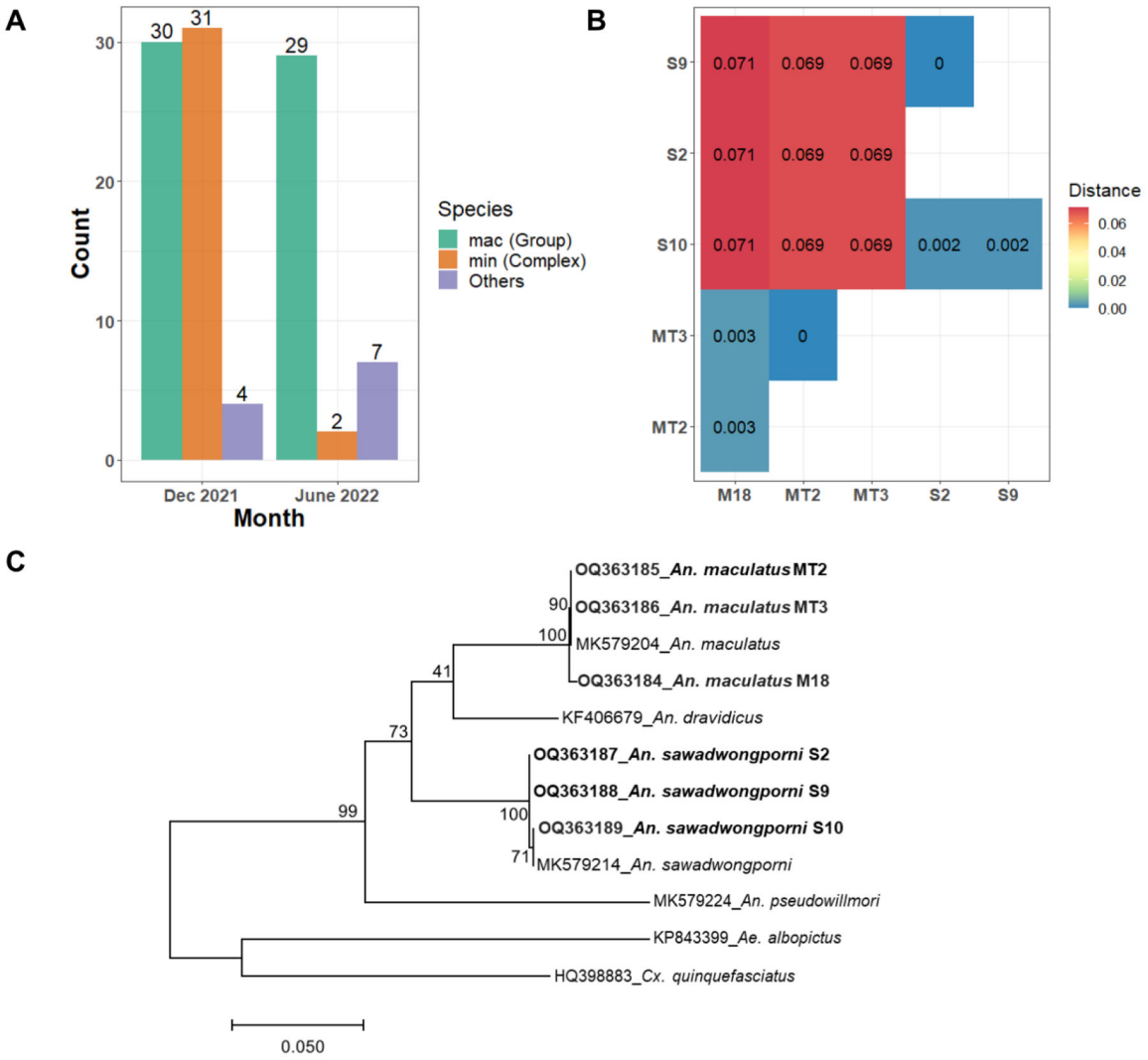

Fig. 1.

Mosquito composition and phylogenetic analyses. (A) *Anopheles* composition captured from Suan Oi village and identified based on morphology. (B) K2P genetic distances of six samples of the Maculatus Group. (C) Maximum likelihood phylogenetic tree of four members of the Maculatus Group based on *cox1* sequences. All sequences generated in this study are presented in bold type. mac (M/MT) indicates *An. maculatus*. saw (S) indicates *An. sawadwongporni*.

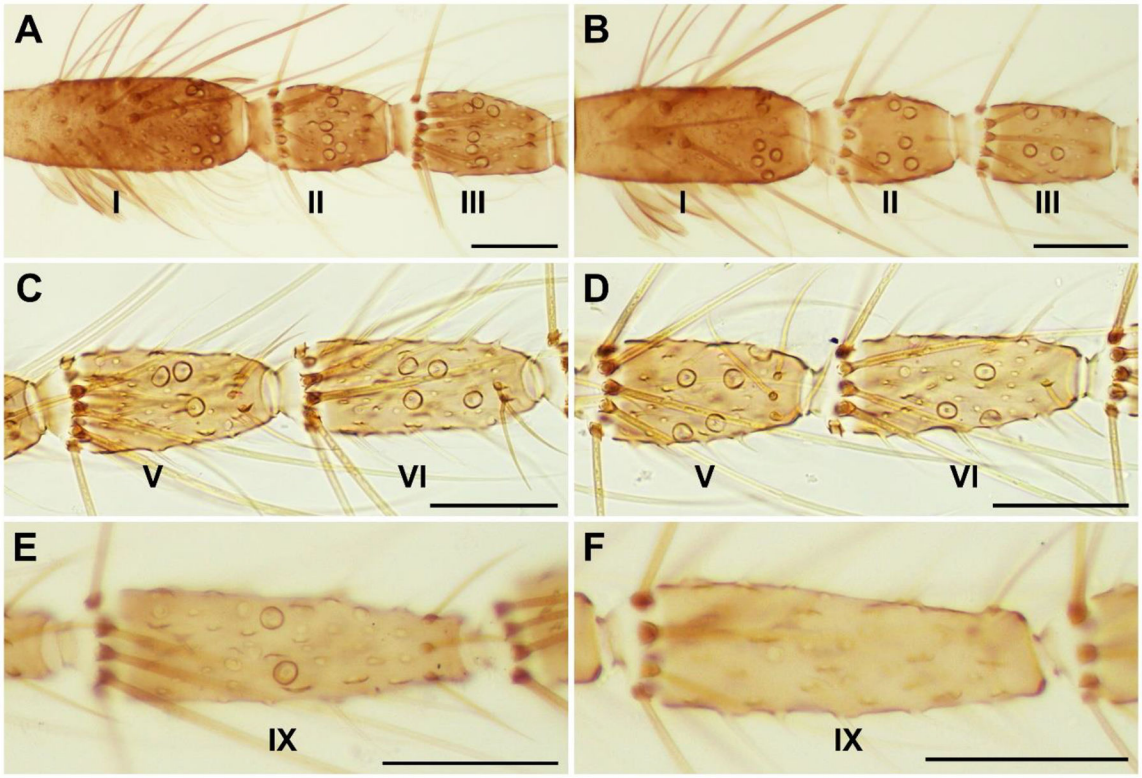

Fig. 2.

Representative images of large coeloconic sensilla housed on flagellomeres 1–3, 5–6 and 9 of female *An. maculatus* (**A, C, E**) and *An. sawadwongporni* (**B, D, F**) under light microscope. Scale bars indicate 50 μm.

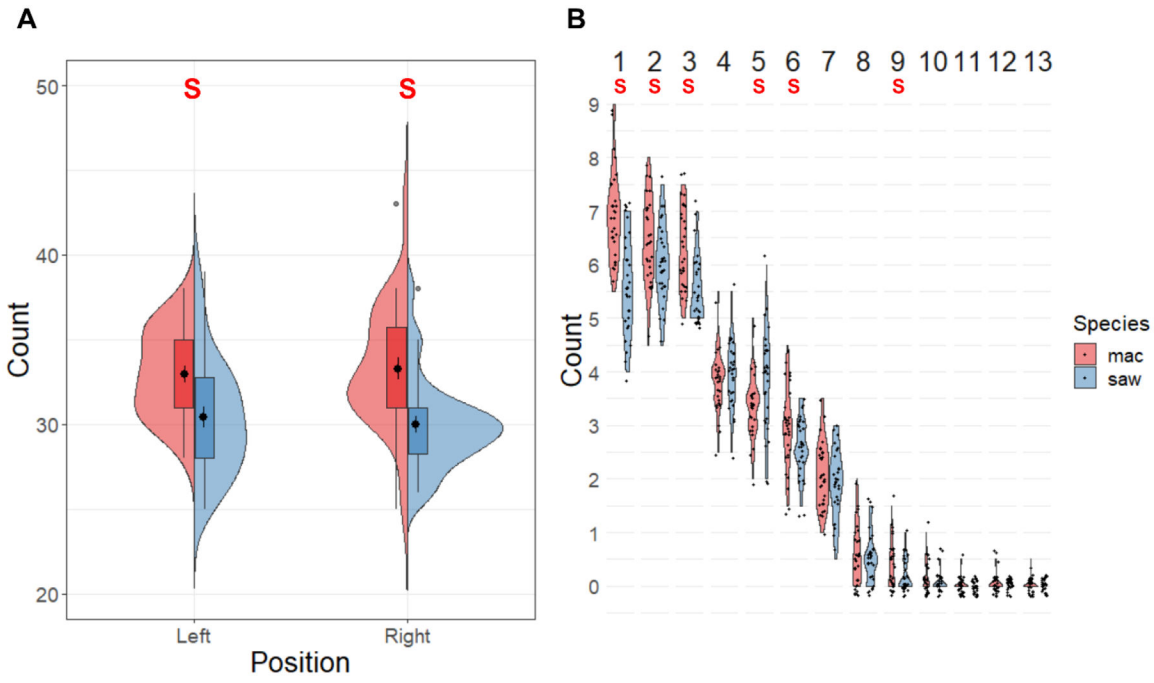

Fig. 3.

The count of KOH-soaked large sensilla coeloconica (lco) on antennae of *An. maculatus* (mac) and *An. sawadwongporni* (saw) under light microscope (n = 60/species). (A) Violin plots overlaid with box plots of lco numbers on left versus right flagellum in mac versus saw. Student's t-test is implemented in this section. S indicates significant difference (p < 0.05). (B) Violin plots of average lco numbers on each flagellomere in mac versus saw. Mann–Whitney U test is implemented in this section. S indicates significant difference (p < 0.05). Statistical test values are provided in the supplementary file (Table S2, S3).

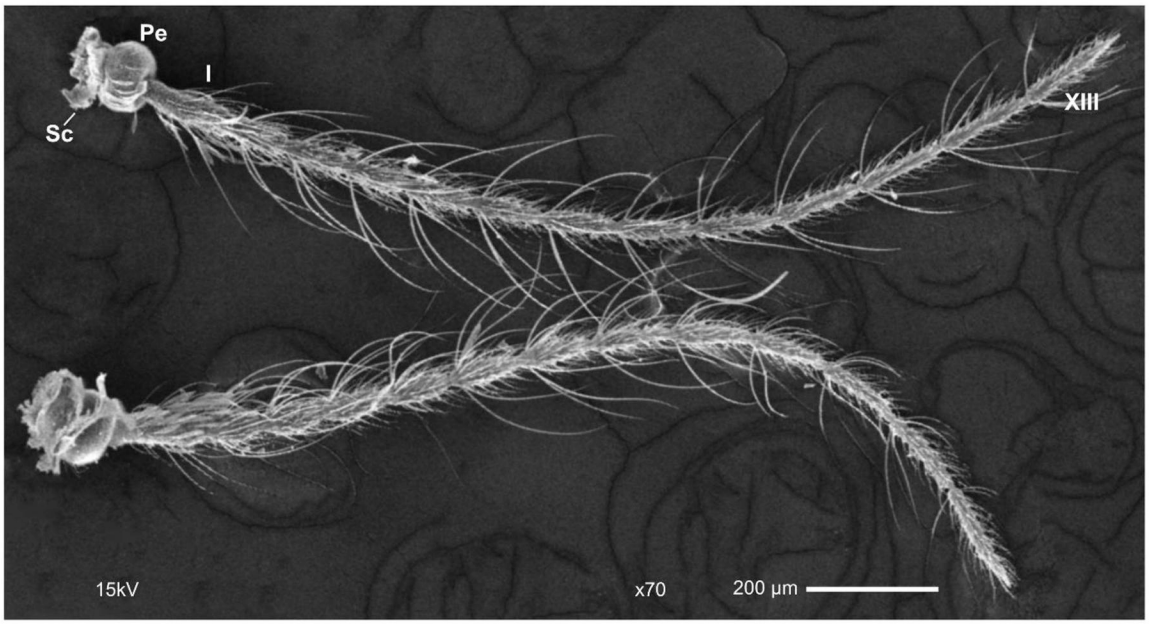

Fig. 4.

Scanning electron micrograph showing the female antennae of *An. maculatus* (virtually identical in *An. sawadwongporni*). Scape (Sc), Pedicel (Pe), Flagellomere 1 (I), and Flagellomere 13 (XIII) are indicated.

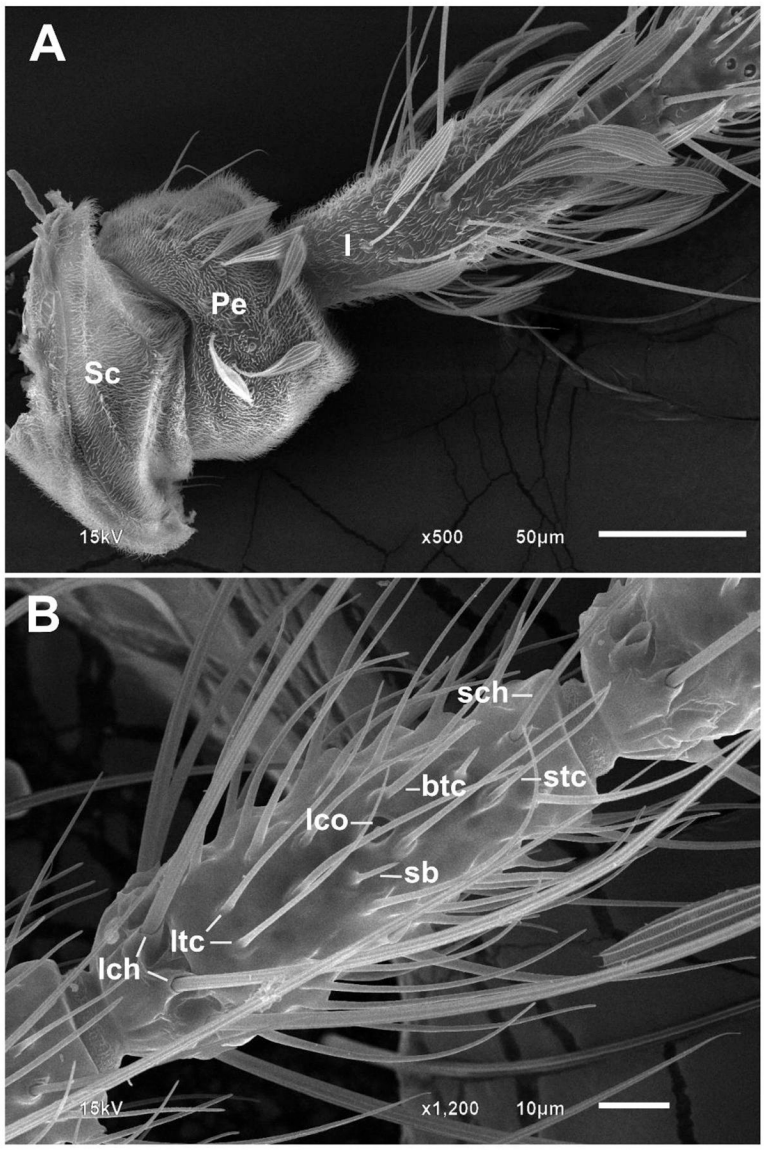

Fig. 5.

Representative scanning electron micrographs of the antenna of female *An. sawadwongporni* (virtually identical in *An. maculatus*). (A) Scanning electron micrograph of Scape (Sc) and Pedicel (Pe) covered with aculeae (ac) and adjacent to flagellomere 1. (B) Sensilla types on flagellomere 5. btc, blunt-tipped sensillum trichodeum; lch, large sensilla chaetica; lco, large sensillum coeloconicum; ltc, long sharp-tipped sensilla trichodea; sb, sensillum basiconicum; sch, small sensillum chaeticum; stc, short sharp-tipped sensillum trichodeum.

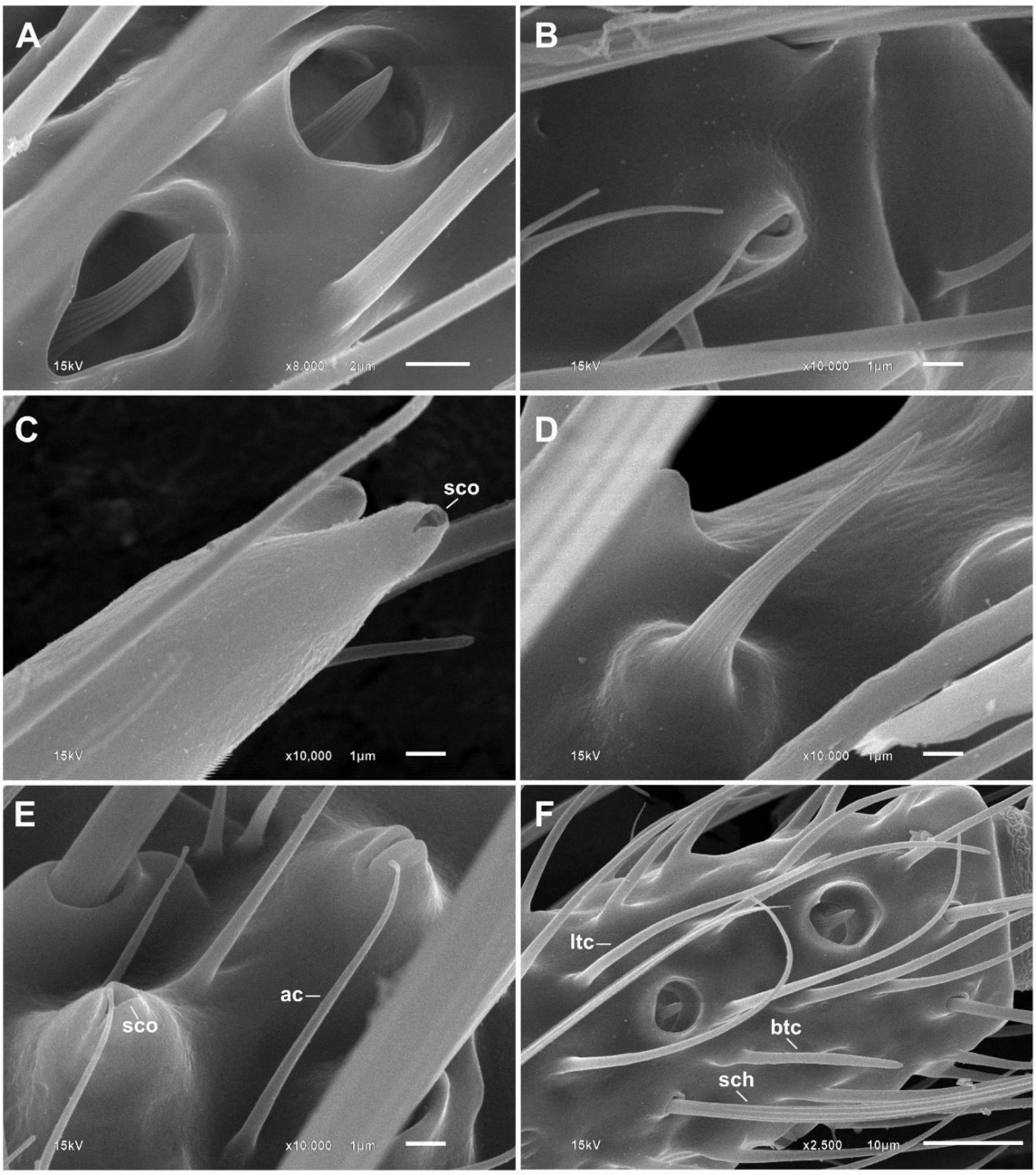

Fig. 6.

Higher magnification of antennal sensilla found in *An. maculatus* and *An. sawadwongporni*. (A) Large sensilla coeloconica. (B) Small sensillum coeloconicum on flagellomere 1. (C) Small sensilla coeloconica (sco) at the tip of flagellomere 13. (D) Sensillum basiconicum (grooved peg). (E) Small sensilla coeloconica surrounded by the aculeae on flagellomere 1. (F) Long sharp-tipped sensillum trichodeum, blunt-tipped sensillum trichodeum, and small sensillum chaeticum on flagellomere 3.

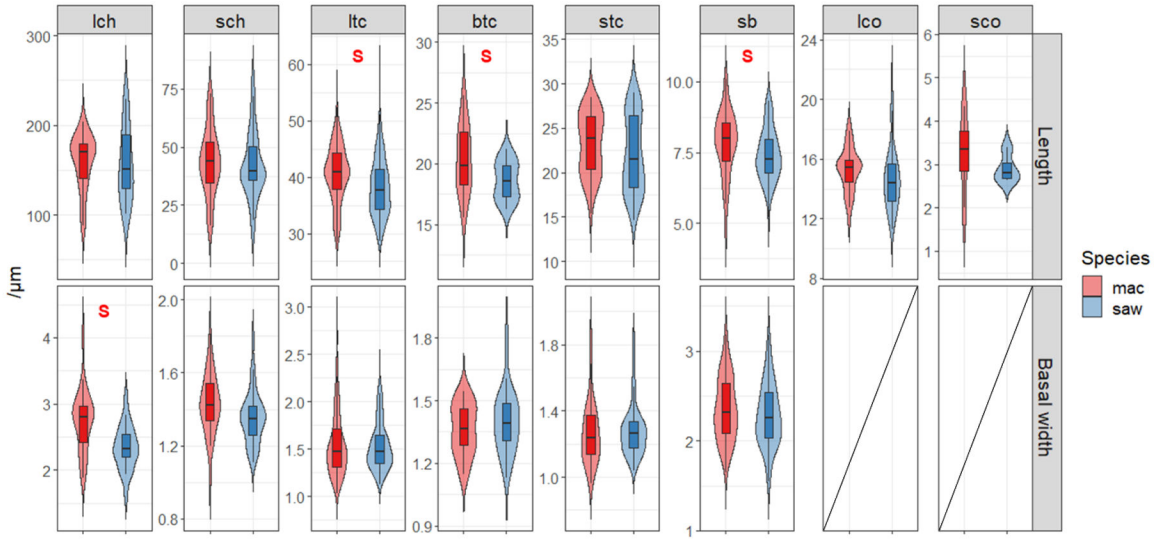

Fig. 7.

Violin plots overlaid with box plots showing the lengths and basal widths of each antennal sensillum from *An. maculatus* (mac) versus *An. sawadwongporni* (saw). Student's t-test and Mann–Whitney U test are implemented in this section. S indicates significant difference ($p < 0.05$). lch = large sensilla chaetica. sch = small sensilla chaetica. ltc = long sharp sensilla trichodea. btc = blunt-tipped sensilla trichodea. stc = short sharp sensilla trichodea. sb = sensilla basiconica. lco = large sensilla coeloconica. sco = small sensilla coeloconica. Statistical test values are provided in the supplementary file (Table S4).